BioTechniques

ISSN: 0736-6205 (Print) 1940-9818 (Online) Journal homepage: www.tandfonline.com/journals/ibtn20

Isolation and profiling of single circulating tumor cells in myeloma: a new workflow for liquid biopsies

Yulia Shifrin , Asieh Alikhah , Zahabiya Husain , Michelle Nguyen , Atacenk Baslik , Darryl Dyck , Silvana Ferreira , Rayan Kaedbey , Sandra Mazzoni & Sabine Mai

To cite this article: Yulia Shifrin , Asieh Alikhah , Zahabiya Husain , Michelle Nguyen , Atacenk Baslik , Darryl Dyck , Silvana Ferreira , Rayan Kaedbey , Sandra Mazzoni & Sabine Mai (2026) Isolation and profiling of single circulating tumor cells in myeloma: a new workflow for liquid biopsies, BioTechniques, 78:1-12, 123-136, DOI: 10.1080/07366205.2026.2645352

To link to this article: https://doi.org/10.1080/07366205.2026.2645352

Published online: 24 Mar 2026.

BIOTECHNIQUES
2026, VOL. 78, NO. 1-12, 123–136
https://doi.org/10.1080/07366205.2026.2645352

Taylor & Francis
Taylor & Francis Group

REPORT

Isolation and profiling of single circulating tumor cells in myeloma: a new workflow for liquid biopsies

Yulia Shifrin[a], Asieh Alikhah[a], Zahabiya Husain[a], Michelle Nguyen[a], Atacenk Baslik[a], Darryl Dyck[b], Silvana Ferreira[c], Rayan Kaedbey[c], Sandra Mazzoni[d] and Sabine Mai[b]

[a]Telo Genomics Corp, Toronto, ON, Canada; [b]University of Manitoba, Winnipeg, MB, Canada; [c]Jewish General Hospital, Montréal, Canada; [d]Cleveland Clinic Foundation, Cleveland, OH, US

ABSTRACT

Minimal residual disease (MRD) is a key prognostic marker for progression-free and overall survival in multiple myeloma (MM). Existing high sensitivity assays primarily focus on tumor burden assessment, rely on bone marrow sampling, and are limited in their ability to support frequent longitudinal disease monitoring. Here, we describe a proof-of-principle workflow for isolating morphologically preserved circulating tumor cells (CTCs) from peripheral blood (PB) using size-based filtration. Based on controlled spiking experiments with RPMI 8226 myeloma cells, we demonstrate an analytical limit of detection of approximately 1 tumor cell per 10^7 white blood cells. Isolated cells retain nuclear integrity and cytomorphology, allowing for downstream immunophenotyping, three-dimensional (3D) telomere fluorescence *in situ* hybridization (FISH), and single-cell telomere profiling, a known marker of genomic instability and disease progression in multiple myeloma. The proposed workflow demonstrated its feasibility for isolating, profiling, and analyzing plasma cells from PB of MM patients at different disease stages. It revealed distinct nuclear and telomeric features in MM CTCs compared with normal lymphocytes. The established technically robust liquid biopsy workflow enables 3D telomere profiling of MM CTCs that can be adopted for noninvasive MRD monitoring based on genomic instability rather than on the enumeration of MM plasma cells alone.

ARTICLE HIGHLIGHTS

- Current high-sensitivity assays for assessing minimal residual disease (MRD) in multiple myeloma (MM) patients rely on invasive bone marrow sampling and are limited by sampling bias and poor suitability for frequent longitudinal monitoring.
- This study presents a proof-of-principle liquid biopsy workflow that enables isolation of morphologically intact circulating tumor cells (CTCs) from peripheral blood (PB) using size-based filtration with the ScreenCell® device.
- Controlled spiking experiments with RPMI 8226 myeloma cells established an analytical limit of detection of approximately 1 tumor cell per 10^7 white blood cells.
- Technical feasibility of the new workflow for isolating intact CTCs from liquid biopsy was confirmed in a cohort of 20 newly diagnosed MM patients at diagnosis, during induction therapy, and after relapse, supporting its potential utility for longitudinal disease monitoring.
- Isolated CTCs were successfully immunophenotyped and subjected to quantitative three-dimensional telomere fluorescence *in situ* hybridization (FISH), allowing single-cell analysis of telomere length, number, aggregation, nuclear volume, and spatial distribution.
- Quantitative telomere profiling revealed statistically significant differences in nuclear and telomeric parameters between MM CTCs and normal lymphocytes, consistent with known markers of genomic instability and disease aggressiveness in MM.
- By combining enumeration with risk assessment based on telomere profiling, the current workflow can provide clinicians with much-needed biological insight beyond mere tumor burden assessment. Incorporating minimally invasive telomere profile-based risk assessment into MRD guidelines may guide treatment decisions in cases of sustained MRD and inform the need for new treatment regimens when residual disease is detected

ARTICLE HISTORY

Received 12 September 2025
Accepted 9 March 2026

KEYWORDS

Minimal Residual Disease; multiple myeloma; three-dimensional telomere analysis; liquid biopsy

CONTACT Yulia Shifrin yulia.shifrin@telodx.com Telo Genomics Corp, Toronto, ON M5V 3B1, Canada.

MULTIDISCIPLINARY ABSTRACT

Multiple myeloma (MM) is an incurable hematological cancer. Minimal residual disease (MRD) is used as a prognostic surrogate marker for progression free survival (PFS) and MRD negativity rate is a common primary endpoint for clinical trials. Current MRD tests are accurate but require invasive bone marrow sampling, which is not ideal for routine monitoring. In this study, we describe a new blood-based method that detects circulating tumor cells (CTCs) in MM patients with higher sensitivity than any reported approach to date. In addition to counting and characterizing these tumor cells, the new method also enables a detailed 3D analysis of their telomeres, which serve as markers of genetic instability and disease progression. This proof-of-principle study demonstrates that MRD can be monitored through a simple blood test, opening the door to less invasive, more informative, and more frequent monitoring for patients with MM that does not rely on an initial diagnostic sample for tracking.

METHOD SUMMARY

We isolated plasma cells from the peripheral blood of multiple myeloma (MM) patients by filtration, based on the principle of size exclusion. Isolated cells were counted and immunophenotyped. 3D telomere profiles of identified MM plasma cells were analyzed and compared to those of normal lymphocytes.

1. Introduction

Multiple myeloma (MM) represents approximately 1% of all cancers and 10% of all hematological malignancies [1]. Novel therapeutic approaches in both front-line and relapsed/refractory settings have significantly increased the median survival of MM patients, with over 70% achieving deep responses with front-line therapy [2–4]. An important marker of disease response is minimal residual disease (MRD), characterized by the presence of detectable clonal plasma cells in bone marrow with sensitivities of 10^{-5} to 10^{-6}. Moreover, given the patchy nature of myeloma's marrow involvement, some patients may have residual disease in sites of marrow that are not accessible through standard biopsy techniques and/or plasmacytomas (which could be extra- or para-medullary). As a result, having a blood-based assay can provide more insight into the disease rather than assessing a single site of bone marrow. Levels of circulating tumor cells (CTCs) in the peripheral blood (PB) of myeloma patients are increasingly recognized as a prognostic biomarker for risk stratification in newly diagnosed MM (NDMM), and have demonstrated a correlation with the MRD negativity rate and PFS in two recent trials [5–10]. Evaluation of CTCs in PB had superior prognostic value compared to quantification of BM PCs, and the threshold of ≥ 0.01% CTCs emerged as a new risk factor in novel staging systems for patients with transplant-eligible MM [8]. CTC levels were also identified as an independent prognostic factor in the context of the most effective standard of care for transplant-eligible NDMM [11]. However, noninvasive detection of MM cells in peripheral blood is not implemented in clinical practice due to a lack of standardization, high costs, labor intensity, and, notably, the absence of clear thresholds for MRD positivity or negativity based on the numbers and/or characteristics of CTCs in the liquid biopsy of MM patients [12,13]. Furthermore, despite significant correlations in CTC levels in the peripheral blood of SMM and MM patients, CTC counts alone are insufficient to describe the disease's dynamics and fail to accurately reflect clonal heterogeneity, including high- and low-risk clones [14].

In this context, single-cell analyses enable a more accurate assessment of clonal diversity and the inherent heterogeneity of MM, as well as the detection of treatment-resistant clones or subpopulations, which are indicative of clonal evolution and aggressiveness [13,15]. Studies have shown that achieving MRD negativity at a sensitivity threshold of 10^{-6} is consistently associated with improved PFS and overall survival (OS) **[**15**,**16**]**. Clinically recognized MRD detection approaches, such as next-generation sequencing (NGS) and multiparametric next-generation flow cytometry (NGF) are based on bone marrow specimens, requiring the invasive marrow aspiration, considerably limiting the ability to monitor patients over time [17–20]. Furthermore, due to the patchy nature of the MM infiltration, bone marrow aspiration introduces a risk of a sampling error that is not observed with liquid biopsy [21–23]. Therefore, developing methods that are based on liquid biopsy, such as cell-free DNA primers to estimate residual cell

number and mass spectrometry to monitor immunoglobulin protein synthesis, has become a focus of attention [24]. Liquid biopsy offers a minimally invasive way to longitudinally monitor disease burden, molecular changes, treatment response, resistance, and emerging therapeutic targets. It is especially beneficial for monitoring precursor, extramedullary, or serologically non-measurable disease. Nevertheless, the sensitivity of liquid biopsy for MRD detection still lags behind that of bone marrow–based assays [24]. Therefore, there is a specific need for standardized methods and more sensitive technologies to expand the clinical utility of blood-based MRD assessment, ultimately supporting more precise risk stratification and individualized care.

Furthermore, isolating intact plasma cells from the PB enables 3D analysis of the malignant cell architecture to identify additional markers of genome instability, such as telomere length and spatial distribution within the nucleus, which have been linked to the progression of several hematological malignancies, including MM [25–30]. Recently, spatial telomere profiling using TeloView, a software specifically designed to quantify key 3D telomeric parameters on a single-cell level, has demonstrated utility in predicting higher risk disease across the spectrum of myeloma, from monoclonal gammopathy of undetermined significance (MGUS) to smoldering MM (SMM), and MM, in a prospective study of 214 patients who were followed for 5 years [25]. Furthermore, TeloView profiling was used to identify NDMM patients developing resistance to first-line therapy and to stratify smoldering MM (SMM) patients by risk of disease progression [31,32]. TeloView identifies and quantifies several crucial parameters of genomic instability, such as the number of telomeres as an indicator of aneuploidy, their length as measured by relative fluorescent intensity, number of aggregates, the spatial distribution of telomeres throughout the cell cycle (axial or *a/c* ratio, with lower *a/c* values indicating spherical nuclei typical of proliferating cells), nuclear volume, and the telomere numbers to the nuclear volume ratio [33].

Here, we describe a new workflow for the efficient isolation of myeloma cells from liquid biopsies and demonstrate through a spiking experiment that the method achieves a limit of detection of 10^{-7}. We then show that the new workflow is adaptable for isolating plasma cells from the PB of MM patients, both at the point of diagnosis (NDMM) and post-treatment/transplantation (MRD). The malignant profile of the isolated CTCs is confirmed by 3D co-immuno-telomere fluorescent in situ hybridization (FISH) and 3D telomere single-cell analysis using the TeloView software platform.

2. Materials and methods

2.1. Cell cultures and patient samples

RPMI 8226 (B lymphocytes from a plasmacytoma patient) cells were purchased from ATCC (Manassas, VA, USA). Cells were cultured in modified RPMI 1640 medium (ATCC**)** containing 2 mM L-glutamine, 10 mM HEPES, 1 mM sodium pyruvate, 4500 mg/L glucose, and 1500 mg/L sodium bicarbonate, supplemented with 10% fetal bovine serum (FBS) and 1% antibiotic/antimycotic solution (Thermo Fisher Scientific, Waltham, MA, USA) in 37 °C, 5% CO_2.

Human PB for the spiking experiment was obtained from a healthy donor. PB for quantitative 3D telomere co-immunofluorescence *in situ* hybridization (FISH) was collected from MM patients enrolled in the MRD clinical trial (NCT05530096) at different points in the course of the treatment: at baseline, on induction, and after relapse. All patients provided written informed consent in accordance with the principles outlined in the Declaration of Helsinki.

2.2. CTC isolation from peripheral blood

CTC isolation from PB of 20 MM patients was performed using the ScreenCell® Cyto devices (ScreenCell, Paris, France) according to the manufacturer's instructions, and as described by Desitter *et al.* [32]. Briefly, 9 mL of whole PB was collected into the TransFix/ethylenediaminetetraacetic acid (EDTA) tube (Cytomark LTD, Buckingham, UK), immediately mixed by inverting the tube 10 times to stabilize venous blood at the point of collection, and incubated at room temperature (RT) for at least 4 hours before further processing. Then, 3 ml of diluted blood sample was incubated with 4 ml of ScreenCell FC2 fixation buffer for 15 min at RT with constant gentle agitation to allow complete lysis of red blood cells (RBCs) and to

preserve nucleated cells. Diluted blood samples were applied to the upper module of the ScreenCell Cyto device, which contains an isolation support (filter) with an 18-µm-thick polycarbonate membrane with circular pores of 6.5 ± 0.33 µm. A mild vacuum force was applied to draw the blood through the filter, and the remaining blood waste was washed off by adding 1.6 mL of Phosphate-Buffered Saline (PBS) 1X (Thermo Fisher Scientific, Waltham, MA, USA) at the end of the filtration. The filter was dislodged from the ScreenCell® Cyto device, rinsed with PBS 1X, and dried on absorbent tissue.

2.3. Sensitivity test of RPMI 8226 cell detection during spiking experiments

The viability of the cultured RPMI 8226cells was first assessed by trypan blue exclusion. Briefly, an aliquot (10 µL) of RPMI 8226 cells was mixed with an equal volume of trypan blue (Sigma-Adrich, St. Louis, MI, USA) and counted under a light microscope. The percentage of viable cells was calculated by dividing the number of trypan blue-unstained cells by the total number of cells and multiplying by 100. Cells were used only when viability exceeded 90%.

The sensitivity of the method was assessed by spiking RPMI 8226 cells into the PB of a healthy volunteer (a white blood cell (WBC) count of 7.5×10^6/mL). The spiked RPMI 8226 cell numbers were estimated at 2, 20, and 200 cells by serial dilution in complete growth medium (final volume of 20 µL). The final white blood cell concentration in the spiking experiment was 6.6 x 10^6/ml. This concentration ensures that each 3 ml of blood contains approximately 2×10^7 cells. The diluted RPMI 8226 cells were spiked into 3 ml of PB (~2×10^7 WBC), immediately incubated with the ScreenCell® FC2 fixation buffer, and processed as described above. The experiment was performed in triplicate.

2.4. Enumeration of captured RPMI 8226 and CTCs

Captured RPMI 8226 cells (spiking experiment) or plasma cells (from MM patients) were visualized by staining the filter with Modified Giemsa Stain (MSG) (Sigma-Adrich, St. Louis, MI, USA) based on the manufacturer's instructions. After staining, filters were attached to the microscope slide with a drop of rubber cement (Elmer's, Toronto, Ontario, Canada). The entire area of the filter was imaged using an AxioImager Z2 microscope (Zeiss, Jena, Germany) using an Epiplan 50x/0.65 d = 0 objective (Zeiss, Jena, Germany). The software used was GenASIs (Applied Spectral Imaging, Carlsbad, CA, USA), utilizing the HiSlide scanning module. The images were acquired at the Nano and Cell Imaging Facility at the University of Manitoba (RRID: SCA_025133) and underwent cytomorphological analysis.

Captured cells were classified as CTC if all 3 of the following cytological criteria were present: 1) Nuclei larger than the 6.8 µm ScreenCell® filter pore size; 2) Eccentrically placed nuclei; and 3) Perinuclear halo. Malignant phenotypes of isolated cells were confirmed by immuno-staining as described below.

2.5. Quantitative 3D telomere co-immuno-FISH assay and image acquisition

Isolation supports were attached to the microscope slide using a drop of rubber cement, followed by Antigen Retrieval (S169984-2, Agilent, Canada) treatment for 30 min at 95 °C. A quantitative 3D-telomere *FISH* hybridization was performed using the Cy-3-labeled PNA telomere probe (Panagene, Daejeon, South Korea) and a ThermoBright machine (Leica Biosystems, Deer Park, IL, USA) as follows: denaturation at 80 °C for 3 min; hybridization at 30 °C for 2 h. The sides were washed twice in washing buffer I (70% Formamide/10 mM Tris pH 7.5 ± 1) at RT for 15 min each and in a washing buffer II (0.1X saline-sodium citrate (SSC, pH: 7.5 ± 1)) for 5 min at 55 °C. Slides were blocked in Super Block buffer (Sigma-Adrich, St. Louis, MI, USA) for 5 min at RT, followed by incubation with a cocktail of Mouse Anti-Human Alexa Fluor® 488-conjugated CD56 antibody (BD Bioscience, San Jose, CA, USA) and Anti-Human Alexa Fluor® 647-conjugated CD138 (Syndecan-1) antibody (Biolegend, San Diego, CA, USA) at a dilution of 1:50, each. After incubation, slides were washed, and the nuclei were counterstained with 4'6 diamidino-2-phenylindole (DAPI), followed by application of antifade mounting medium Vectashield (Vector Laboratories, Burlington, Ontario, Canada).

Images were acquired using a Zeiss Axio Imager Z.2 microscope (Zeiss, Jena, Germany) equipped with a Hamamatsu digital camera (C11440-42 U). Eighty-one focal planes spaced at 200 nm were captured along the *Z*-axis (specimen depth) for every fluorochrome, including Cy3 filter (telomeres) at 100 ms,

Spectrum green (CD56) at 350 ms, Cy5 (CD138) at 250 ms, and DAPI (DNA) at 10–20 ms. Images of individually selected cells were then processed using the constrained iterative deconvolution algorithm (Zeiss) to reconstruct a 3D image using the acquired 81 focal planes.

2.6. TeloView® analysis

Telomere parameters were quantified in 3D using the TeloView® software platform [33] that quantifies six primary molecular and structural telomeric parameters including: (1) telomere length as a function of signal intensity; (2) number of telomere signals/nucleus; (3) number of telomeric aggregates (clusters of telomeres that are too close to be further resolved at an optical resolution limit of 200 nm); (4) nuclear volume; (5) *a/c* ratio (spatial feature that assesses cell cycle progression and is a measure of proliferation and cell cycle progression); and (6) the distribution of telomeres within the nuclear space (spatial feature that informs on gene expression).

2.7. Statistical analysis

Univariate paired analyses were used to compare specific nuclear and signal-based features of 25 myeloma CTCs and 25 lymphocytes within individual patients. Two complementary approaches were used to evaluate feature-level differences.

First, a randomized block ANOVA was applied to individual cell-level measurements, with cell type (myeloma CTCs vs. lymphocytes) as the fixed effect and case (patient ID) as a blocking factor. This model tested for the main effect of cell type, as well as the interaction between case and cell type. Type III sum of squares was used, and the Case × Cell Type interaction term served as the error term for hypothesis testing. This analysis accounts for within-patient pairing and was used to assess the consistency of cell-type differences across the cohort.

Second, to reduce the influence of inter-cell variability and potential interaction effects, a paired analysis of case-level summary statistics was conducted. For each feature and patient, five descriptive metrics were computed: 25th percentile, median (50th percentile), 75th percentile, mean, and interquartile range (IQR). Paired comparisons of these aggregated values between myeloma CTCs and lymphocytes were performed using general linear models (GLMs) with repeated measures. Significance was defined at $p < .05$. SAS (version 8.5.0.203) was used for all statistical testing.

3. Results and discussion

3.1. Isolation of plasma cells by size-based filtration improves the limit of detection

The ScreenCell® filtration device allows the isolation of CTCs from 3 mL of patients' blood based on the principle of size exclusion (35), where only cells larger than the pore size of the microporous membrane filter (6.5 ± 0.3 µm) are retained. This approach does not rely on the expression of specific cell surface antigens, allowing for the assessment of the total CTC population, which is particularly important in highly heterogeneous diseases, such as MM.

However, this method of CTC isolation is currently applied to solid tumors, such as melanoma, prostate, lung, colon, breast cancers, etc [34–37]. To assess the sensitivity of the ScreenCell® Cyto device for the detection of CTCs in MM, 3 mL PB from a healthy donor, diluted to 2×10^7, was spiked with 2, 20, and 200 RPMI 8226 cells (for the LODs of 1×10^{-7}, 1×10^{-6}, and 1×10^{-5}, respectively; Figure 1A, B). RPMI 8226 cells spiked into the complete medium were used as a control (Figure 1C). We meticulously ensured that the exact number of cells (±20%) was added to each PB sample. MGS-stained RPMI 8226 cells on the IS were identified based on morphology and enumerated (Figure 1).

The results of the spiking experiment are summarized in Figure 2 and Table 1. Regression analysis of observed versus expected counts yielded a slope of 1.01 [95% CI, 0.85–1.17], an intercept of 0.07 (95% CI, −18.3 to 18.4), and a coefficient of determination R^2 of 0.97. As expected, the coefficient of variation increased at lower spike levels, ranging from 16.6% at the 200-cell spike to 24.7% at the 2-cell spike (13.2% at 20 cells). The average percentage of recovered RPMI 8226 cells was approximately 100% at the

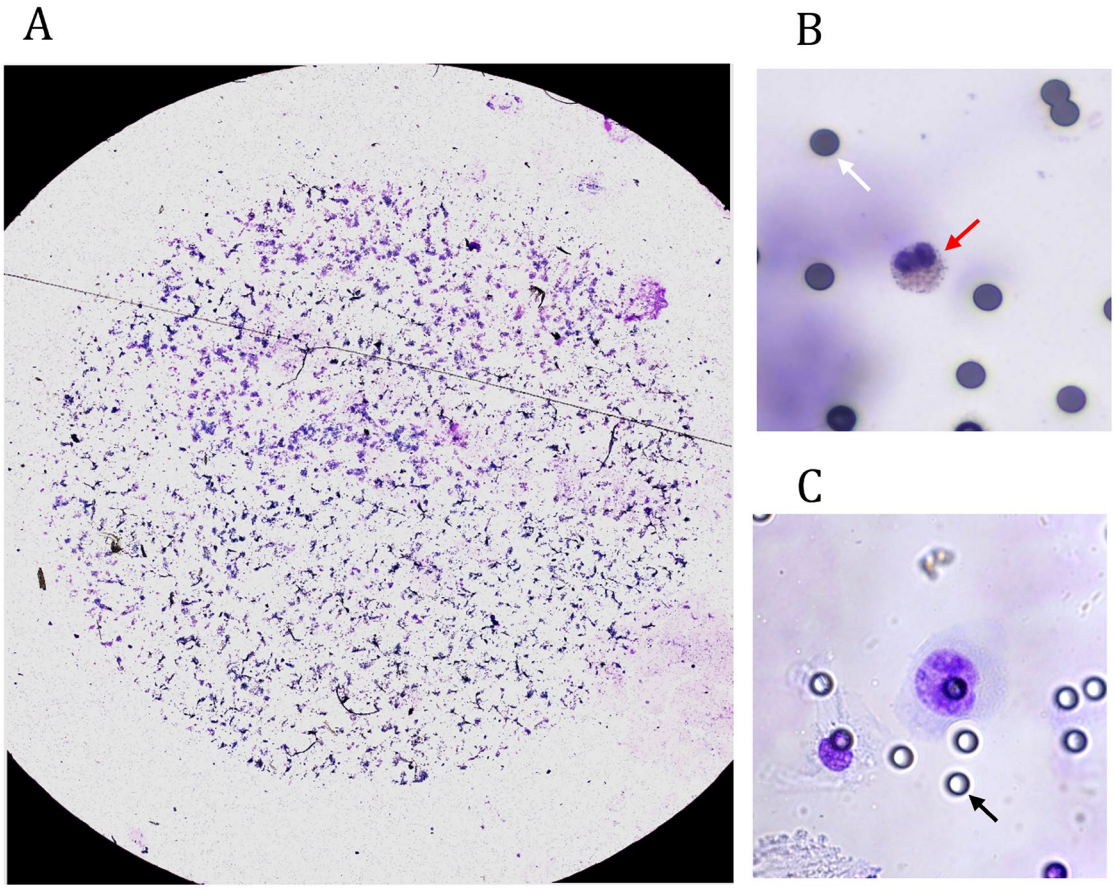

Figure 1. (A) Isolation support, stained with modified Giemsa stain; (B) RPMI 8226 cell (red arrow), spiked into the whole blood; white arrow: normal lymphocyte inside the pore; (C) Captured RPMI 8226 cell, spiked into the complete growth medium; black arrow: pore.

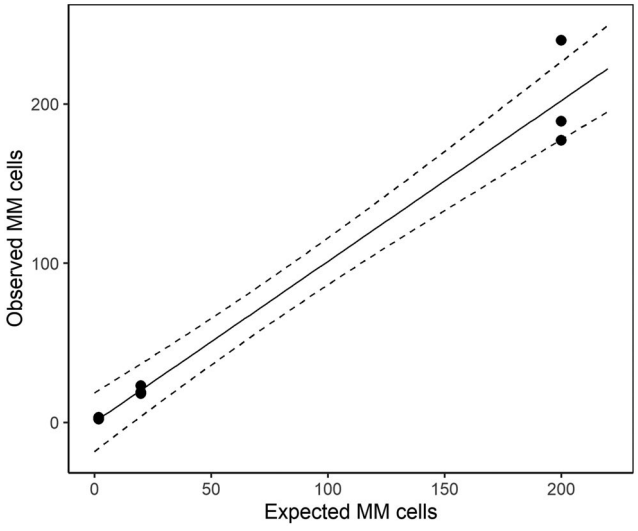

Figure 2. The expected number of RPMI 8226 MM cells spiked (2, 20, or 200 cells) was plotted against the actual number of cells observed.

20- and 200-cell levels and 116.7% at the 2-cell level. At the lowest spike level (2 cells), at least two cells were detected in all three samples. The estimated recovery was near 100% for all spike levels, which corresponds to approximately 1 RPMI 8226 cell in 10^7 white blood cells.

Table 1. Determining the limit of detection by spiking experiment.

Expected # of MM cells	Observed # of MM cells			% Recovery		
	Average	SD	95% CI	Average	95% CI	%CV
2	2.3	0.6	0.9–3.8	116.7	45–188.4	24.7
20	20	2.6	13.4–26.6	100	67.1–132.9	13.2
200	202	33.5	118.9–285.1	101	59.5–142.5	16.6

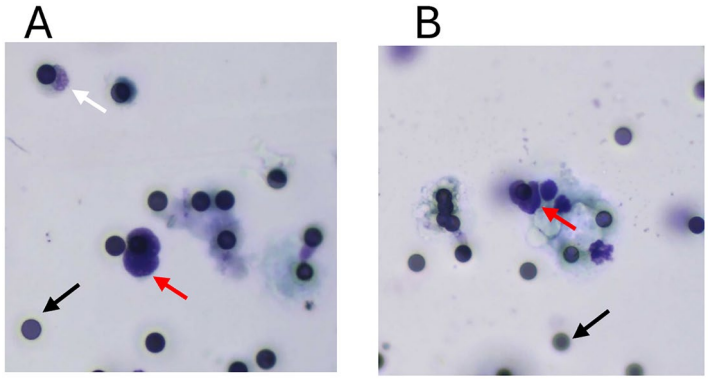

Figure 3. CTCs in the peripheral blood of an MM patient at the point of diagnosis (A), and at 3 months post-ASCT (B). Red arrows: CTCs; Black arrows: IS pore; White arrow: normal lymphocyte.

Table 2. Enumeration of plasma cells isolated from the peripheral blood of MM patients.

Time point	Number of patients	Average plasma cell count/ filter (±SD)	Average whole blood cell count/filter (±SD)	Average whole blood cell count/cohort (±SD)
Diagnosis	10	67.7 (±32.3)	2.16 (±0.3) x 10^7	2.03 (± 0.83) x 10^7
Induction	6	10 (±7.1)	1.7 (±1.1) x 10^7	
Relapse	4	33.6 (±21.2)	2.07 (±1.2) x 10^7	

These results demonstrate that the method of size-based filtration of whole blood allows the achievement of a LOD of 1 x 10^{-7} (one plasma cell in 10 million blood cells).

Notably, compared to RPMI 8226 cells spiked into complete medium (Figure 1C), RPMI 8226 cells, spiked into whole blood, demonstrated signs of stressed morphology, such as cell membrane blebbing and vacuolization (Figure 1B). These changes confirm the previously reported fragility of cultured cells in whole-blood settings due to the blood's inherent immune response [38,39]. The standard chemotherapy involved in a common first-line MM regimen,lenalidomide and bortezomib, were shown to impact the morphology of MM cells and promote cell apoptosis [40]. Therefore, the ability of the proposed new method of plasma CTCs isolation to capture and enumerate intact fragile plasma cells in the blood of patients after treatment is expected to have significant clinical relevance.

3.2. Clinical feasibility of the CTC isolation using size-based filtration

Our *in vitro* results demonstrated that MM cells can be isolated from whole blood by filtration, with a LOD of 1×10^{-7} in controlled spiking experiments. These results suggest that the new workflow may have potential clinical value in MRD assessment, comparable or superior to currently available methods, such as ClonoSEQ ® and EuroFlow®, which have a technical LOD of 1×10^{-6}, and a median LOD of 2.9×10^{-6}, respectively [5,41].

We next investigated the technical feasibility of the approach for isolating CTCs from the liquid biopsy of MM patients. Similar to the previous spiking experiment, CTCs were isolated from 3 ml of liquid biopsies from 20 MM patients at the point of diagnosis, at induction, and after relapse. As illustrated in Figure 3, intact plasma cells were identified by MGS staining. As summarized in Table 2, the proposed workflow allowed for the identification of plasma cells at every treatment point, with an average of 67.7 (±32.3), 10 (±7.1), and 33.6 (±21.2) plasma cells per approximately 2.07×10^7 whole blood cells at

diagnosis, induction, and relapse, respectively. The proposed method, therefore, allows for isolating CTCs from the liquid biopsies of MM patients with high sensitivity.

3.3. Identification and telomere profiling of myeloma CTCs isolated by filtration

Cancer cells commonly exhibit altered telomere characteristics, such as the number of telomeres per cell nucleus, telomeric aggregation, and different spatial distribution within the nuclear space [42–45]. These unique 3D telomere profiles emerged as a reliable predictive marker of disease progression in multiple cancers, including MM [25,46–48]. In MM, differential telomere parameters allow the identification of patients with stable or progressive disease and stratification into high-risk versus low-risk. 3D telomere profiling using the TeloView technology was used to develop a risk-stratification model for the risk of progression in patients with smoldering MM [31]. In NDMM patients, the telomere profile was identified as an accurate prognostic biomarker to predict the risk of developing drug resistance to first-line therapy [49].

However, as opposed to the currently available assessment methods, such as NGS and NGF, telomere profiling requires preserved cell morphology and nuclear integrity.

Previous research reported that cells, isolated onto ScreenCell® filters, exhibit a well-preserved morphology, with undamaged nuclear and cytoplasmic contents and membranes [32]. We next assessed the applicability of the described method of CTC isolation for 3D telomere profiling. Of the initial cohort of 20 MM patients, plasma cells of 10 NDMM patients at the point of diagnosis were isolated, underwent 3D-telomere *FISH* hybridization with a Cy3-labeled PNA telomere probe, and immunostained with anti-CD56 and anti-CD138 antibodies. MM CTCs were identified on the isolation supports by positive cytoplasmic co-immunostaining, specific to MM plasma cells (Figure 4). 3D telomere profiles of the selected co-immunostained MM CTCs and normal white blood cells, identified by the absence of specific CD56/CD138 staining, were then analyzed by TeloView®. As shown in Table 3, the paired analysis of case-level aggregated data identified a consistent and statistically significant difference between the two cell types across multiple parameters. Features related to nuclear morphology and spatial organization showed strong separation, with myeloma CTCs demonstrating 1) Increased nuclear volume (25th, 50th, and 75th percentiles; $p = 0.0002–0.0006$) with a larger nuclear volume IQR ($p = 0.0015$), reflecting morphological heterogeneity; 2) Elevated a/c ratio ($p = 0.0025–0.0073$), a marker of nuclear shape and cell cycle state; 3) A greater average distance to nuclear center ($p = 0.0008–0.0039$), indicative of altered chromatin structure, and 4) Lower average intensity (25th, 50th, and 75th percentiles; $p = 0.0046–0.0323$) with no significant differences in IQR.

We were able to demonstrate that size-based filtration preserves the 3D structure of the nucleus, allowing for the analysis of the spatial distribution of telomeres within the nuclear space. The TeloView analysis identified parameters specific to MM CTCs, different from the normal cell population.

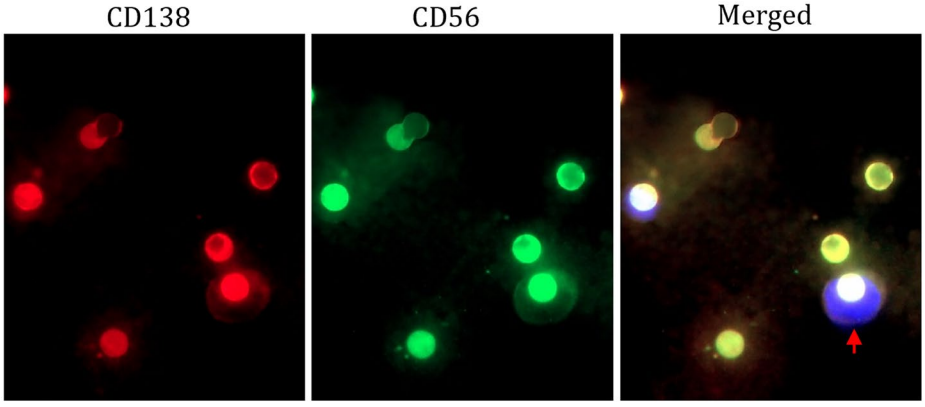

Figure 4. Immunophenotyping of MM CTCs. Representative two-dimensional images of MM CTC (red arrow), captured on the isolation support, and labeled with CD138 (red) and CD56 (green) antibodies; cell nuclei are counterstained with DAPI (blue).

Table 3. Differences between 3D telomere profiles of the MM CTCs and normal lymphocytes.

Telomere parameter	25th percentile value (*p*)	Median (50th percentile) value (*p*)	75th percentile value (*p*)	Mean (*p*)	IQR (*p*)
Nuclear volume	0.0006	0.0004	0.0002	0.0006	0.0015
a/c ratio	0.0073	0.0054	0.0025	0.0057	0.0071
Distance to the nuclear center	0.0008	0.0031	0.0023	0.0039	0.5382
Average signal intensity	0.0323	0.0218	0.0263	0.0046	0.1769
Total signal intensity	0.4784	0.2982	0.2422	0.6138	0.2637
Total # of signals	0.3591	0.3038	0.1745	0.1885	0.2732
Total # of aggregates	0.6521	0.385	0.4418	0.385	0.2406

Paired analysis using general linear models on case-level aggregated features.

4. Conclusion

The results of this proof-of-principle study demonstrated that size-based filtration allows isolation of morphologically preserved CTCs from the liquid biopsies of MM patients with high sensitivity and specificity. To the best of our knowledge, this is the first study reporting the isolation of CTCs from liquid biopsy using the ScreenCell device in a hematological cancer.

Several well-established technologies, such as CellSearch and the Epic Platform, are currently used for circulating tumor cell isolation and enumeration in different cancers, including MM [14,50]. CellSearch relies on immunomagnetic enrichment with antibody-coated ferrofluid beads targeting tumor-associated surface markers [51]. However, the application of magnetic forces imposes physical constraints on the cell surface and the nucleus, altering three-dimensional nuclear organization and making CellSearch-isolated cells unsuitable for downstream telomere profiling. The Epic Platform is based on marker-independent enrichment through red blood cell lysis and centrifugation, followed by plating of millions of nucleated cells onto proprietary glass slides as a monolayer [52]. In the context of spatial nuclear assessment, the combination of centrifugation and enforced planar adhesion alters nuclear shape and spatial chromatin organization, making this approach not compatible with single-cell analysis of nuclear architecture. In contrast, the size-based filtration workflow described here isolates intact plasma cells directly from whole blood without immunomagnetic labeling, centrifugation, or forced adhesion to planar substrates. Cells are retained within a porous membrane, preserving nuclear volume, shape, and internal spatial relationships, enabling quantitative single-cell nuclear analysis that is not achievable with existing clinically established CTC platforms. This ability to perform spatial telomeric analysis on liquid biopsy–derived myeloma cells represents a significant technical advance. Notably, it demonstrates the technical feasibility of combining highly sensitive CTC isolation with quantitative 3D nuclear analysis in MM.

Expanding 3D spatial quantification of nuclear and telomeric features in MM CTCs to assess telomeric dysfunction and genomic instability may enable the development of an MRD scoring model to predict disease relapse. Most existing MRD methodologies do not retain intact cellular and nuclear structures and rely on clinical, cytogenetic, tumor burden, and immune-related biomarkers [53,54], magnetic resonance imaging [55,56], as well as flow cytometry and principal component analysis-based automated detection [57]. The new workflow may be viewed as complementary to existing methods that excel at large-scale enumeration, supporting future development of liquid biopsy–based MRD assessment strategies that extend beyond cell counting to incorporate structural and spatial biomarkers of disease aggressiveness. It provides a foundation for developing complementary MRD assessment strategies that capture genomic instability and clonal heterogeneity from peripheral blood. While the analytical LOD achieved in spiking experiments exceeds that reported for current marrow-based MRD technologies, further research is still needed to determine whether it is clinically equivalent or superior. Our subsequent study will use large prospective and retrospective cohorts to directly compare the size-based CTC isolation and 3D nuclear/telomeric profiling approach with established bone marrow–based MRD methodologies, including next-generation flow cytometry (NGF) and next-generation sequencing (NGS), to determine relative sensitivity, clinical concordance, and prognostic value of the new method.

Preliminary results of the TeloView analysis of telomere profiles for MM MRD demonstrated concordance between blood and marrow in 5 out of 6 parameters in a small cohort of 8 patients, and concordance of all 6 parameters in 6 out of the 8 patients [58]. A study by Klewes *et al.*, comparing blood and bone marrow in 86 patients (MGUS, MM, and relapsed MM), also showed concordance of

telomere profiles for blood and bone marrow for all patients and distinct profiles for each group [27]. We anticipate that combining spatial telomere analysis with existing methods will enable higher-risk MM MRD prediction than either method alone. Future prospective studies will be required to define clinically relevant thresholds, assess concordance with established MRD assays, and determine the prognostic value of telomere-based profiling in longitudinal MM monitoring.

To summarize, the described proof-of-principle workflow presents a new generation of continuous MRD monitoring that assesses genomic instability rather than relying solely on the enumeration of MM plasma cells. The new workflow is based on the isolation and analysis of MM CTCs from liquid biopsy. It may potentially contribute to disease assessment in NDMM patients, as well as to determining MRD status in MM patients at every point in treatment.

5. Future perspective

Future work will include prospective and retrospective clinical trials to test the applicability of the new workflow for determining the MRD status of MM patients and to develop a scoring model for predicting the risk of relapse.

Further research is also needed to address the limitations of this study. First, the reported LOD was determined using controlled spiking experiments with a cultured myeloma cell line in healthy donor blood, which may not fully capture the biological and phenotypic heterogeneity of residual malignant CTCs in treated patients. Second, the small sample size of the clinical cohort does not allow for accurate assessment of clinical sensitivity, specificity, or prognostic performance of the proposed workflow. Finally, while statistically significant differences in telomeric and nuclear parameters were observed between MM CTCs and lymphocytes, larger longitudinal studies are needed to validate the biological and clinical implications of individual telomeric parameters. Importantly, our findings should be interpreted as technical and methodological advances rather than definitive clinical validation of a blood-based MRD assay.

Another critical shortcoming of this study is its reliance on a limited panel of CD56 and CD138 antibodies for immunophenotyping MM CTCs. Recent studies show that some circulating clonal B-cells in MM do not express CD138 [59,60]. Furthermore, the expression of the main surface markers, such as CD138, is downregulated in MRD cells due to the drug treatment, compromising its value as a marker for MRD detection [61]. We are planning to expand the MRD detection panel by incorporating antibodies against B-cell Maturation Antigen (BCMA), a valuable biomarker for monitoring MRD that has almost 100% expression on the surface of normal and clonal plasma cells [62], and CD38, a glycoprotein with ectoenzymatic functions, which is abundantly expressed on myeloma plasma cells [63]. Expanding the panel will further improve the LOD of the new workflow and reduce the risk of misidentification or underestimation of patients' MRD status. We suggest that, by combining enumeration with risk assessment based on telomere profiling, the current workflow can provide clinicians with the much-needed biological insight beyond mere tumor burden assessment. Incorporating minimally invasive telomere profile-based risk assessment into MRD guidelines may guide treatment decisions in cases of sustained MRD and inform the need for new treatment regimens when residual disease is detected.

Acknowledgments

The authors wish to thank the Nano and Cell Imaging Facility at the University of Manitoba (RRID: SCA_025133) for assisting with image acquisition of cells on the isolation supports; Dr. Svetlana Frenkel for helping with the statistical analysis of the data.

Author contributions

CRediT: **Yulia Shifrin**: Conceptualization, Data curation, Formal analysis, Investigation, Methodology, Supervision, Validation, Visualization, Writing – original draft, Writing – review & editing; **Asieh Alikhah**: Data curation, Methodology; **Zahabiya Husain**: Data curation, Methodology; **Michelle Nguyen**: Data curation, Methodology;

Atacenk Baslik: Data curation, Methodology; **Darryl Dyck**: Methodology, Software; **Silvana Ferreira**: Data curation, Project administration; **Rayan Kaedbey**: Methodology, Resources, Writing – review & editing; **Sandra Mazzoni**: Methodology, Resources, Writing – review & editing; **Sabine Mai**: Conceptualization, Investigation, Supervision, Validation, Writing – review & editing.

Disclosure statement

Yulia Shifrin, Asieh Alikhah, Zahabiya Husain, and Atacenk Baslik are employed by Telo Genomics. Sabine Mai is a current equity holder in Telo Genomics. The authors have no other relevant affiliations or financial involvement with any organization or entity with a financial interest in or financial conflict with the subject matter or materials discussed in the manuscript apart from those disclosed.

No writing assistance was utilized in the production of this manuscript.

Ethical declaration

Blood samples were obtained from patients enrolled in the MRD clinical trial NCT05530096. All patients provided written informed consent in accordance with the principles outlined in the Declaration of Helsinki.

Reviewer disclosures

Peer reviewers on this manuscript have no relevant financial or other relationships to disclose.

Funding

The study was sponsored by Telo Genomics, Toronto, Ontario, Canada. The funders had no role in study design, data collection and analysis, decision to publish, or preparation of the manuscript. The work was funded by the Canada Research Chairs; Telo Genomics; Telo Genomics Corp.

Data availability statement

The data that support the findings of this study are available from the corresponding author, Yulia Shifrin, upon reasonable request.

References

Papers of special note have been highlighted as either of interest (*) or of considerable interest (**) to readers.

[1] Siegel RL, Miller KD, Jemal A. Cancer statistics, 2018. CA Cancer J Clin. 2018;68(1):7–30. doi:10.3322/caac.21442

[2] Kristinsson SY, Anderson WF, Landgren O. Improved long-term survival in multiple myeloma up to the age of 80 years. Leukemia. 2014;28(6):1346–1348. doi:10.1038/leu.2014.23

[3] Kumar SK, Dispenzieri A, Lacy MQ, et al. Continued improvement in survival in multiple myeloma: changes in early mortality and outcomes in older patients. Leukemia. 2014;28(5):1122–1128. doi:10.1038/leu.2013.313

[4] Landgren O, Iskander K. Modern multiple myeloma therapy: deep, sustained treatment response and good clinical outcomes. J Intern Med. 2017;281(4):365–382. doi:10.1111/joim.12590

[5] Paiva B, Puig N, Cedena M-T, et al. Measurable residual disease by next-generation flow cytometry in multiple myeloma. J Clin Oncol. 2020;38(8):784–792. doi:10.1200/JCO.19.01231

[6] Jelinek T, Bezdekova R, Zihala D, et al. More than 2% of circulating tumor plasma cells defines plasma cell leukemia–like multiple myeloma. J Clin Oncol. 2023;41(7):1383–1392. doi:10.1200/JCO.22.01226

[7] Termini R, Žihala D, Terpos E, et al. Circulating tumor and immune cells for minimally invasive risk stratification of smoldering multiple myeloma. Clin Cancer Res. 2022;28(21):4771–4781. doi:10.1158/1078-0432.CCR-22-1594

[8] Garcés J-J, Cedena M-T, Puig N, et al. Circulating tumor cells for the staging of patients with newly diagnosed transplant-eligible multiple myeloma. J Clin Oncol. 2022;40(27):3151–3161. doi:10.1200/JCO.21.01365

[9] Ikeda D, Terao T, Oura M, et al. Analysis of baseline circulating tumor cells integrated with PET/CT findings in transplant-ineligible multiple myeloma. Blood Adv. 2024;8(1):37–46. doi:10.1182/bloodadvances.2023011890

[10] Kostopoulos IV, Ntanasis-Stathopoulos I, Rousakis P, et al. Low circulating tumor cell levels correlate with favorable outcomes and distinct biological features in multiple myeloma. Am J Hematol. 2024;99(10):1887–1896. doi:10.1002/ajh.27414
[11] Bertamini L, Fokkema C, Rodríguez-Otero P, et al. Circulating Tumor Cells As a Biomarker to Identify High-Risk Transplant Eligible Myeloma Patients Treated with Bortezomib, Lenalidomide and Dexamethasone with or without Daratumumab during Induction/Consolidation, and Lenalidomide with or without Daratumumab during Maintenance: Results from the Perseus Study. Blood. 2024;144(Supplement 1):487–487. doi:10.1182/blood-2024-199550**This article highlights the prognostic value of CTCs in Multiple Myeloma*
[12] Mailankody S, Korde N, Lesokhin AM, et al. Minimal residual disease in multiple myeloma: bringing the bench to the bedside. Nat Rev Clin Oncol. 2015;12(5):286–295. doi:10.1038/nrclinonc.2014.239
[13] Medina-Herrera A, Sarasquete ME, Jiménez C, et al. Minimal residual disease in multiple myeloma: past, present, and future. Cancers (Basel). 2023;15(14):3687. doi:10.3390/cancers15143687
[14] Vigliotta I, Solli V, Armuzzi S, et al. Circulating Multiple Myeloma Cells (CMMCs) as Prognostic and Predictive Markers in Multiple Myeloma and Smouldering MM Patients. Cancers (Basel). 2024;16(17):2929. doi:10.3390/cancers16172929
[15] Munshi NC, Avet-Loiseau H, Rawstron AC, et al. Association of minimal residual disease with superior survival outcomes in patients with multiple myeloma: a meta-analysis. JAMA Oncol. 2017;3(1):28–35. doi:10.1001/jamaoncol.2016.3160
[16] Munshi NC, Avet-Loiseau H, Anderson KC, et al. A large meta-analysis establishes the role of MRD negativity in long-term survival outcomes in patients with multiple myeloma. Blood Adv. 2020;4(23):5988–5999. doi:10.1182/bloodadvances.2020002827
[17] Rustad EH, Boyle EM. Monitoring minimal residual disease in the bone marrow using next generation sequencing. Best Pract Res Clin Haematol. 2020;33(1):101149. doi:10.1016/j.beha.2020.101149
[18] Kim H-Y, Yoo IY, Lim DJ, et al. Clinical utility of next-generation flow-based minimal residual disease assessment in patients with multiple myeloma. Ann Lab Med. 2022;42(5):558–565. doi:10.3343/alm.2022.42.5.558
[19] Flores-Montero J, Sanoja-Flores L, Paiva B, et al. Next Generation Flow for highly sensitive and standardized detection of minimal residual disease in multiple myeloma. Leukemia. 2017;31(10):2094–2103. doi:10.1038/leu.2017.29
[20] Foureau DM, Paul BA, Guo F, et al. Standardizing clinical workflow for assessing minimal residual disease by flow cytometry in multiple myeloma. Clin Lymphoma Myeloma Leuk. 2023;23(1):e41–e50. doi:10.1016/j.clml.2022.10.008
[21] Kubaczková V, Sedlarikova L, Bollová B, et al. Liquid biopsies-the clinics and the molecules. Klin Onkol. 2017;30(Supplementum2):13–20. doi:10.14735/amko20172S13
[22] Lee N, Moon S, Lee J, et al. Discrepancies between the percentage of plasma cells in bone marrow aspiration and BM biopsy: Impact on the revised IMWG diagnostic criteria of multiple myeloma. Blood Cancer J. 2017;7(2):e530-e530–e530. doi:10.1038/bcj.2017.14
[23] Gozzetti A, Bocchia M. Liquid biopsy and blood-based minimal residual disease evaluation in multiple myeloma. Oncol Res. 2023;31(3):271–274. doi:10.32604/or.2023.028668
[24] Li S, Zhang E, Cai Z. Liquid biopsy by analysis of circulating myeloma cells and cell-free nucleic acids: a novel noninvasive approach of disease evaluation in multiple myeloma. Biomark Res. 2023;11(1):27. doi:10.1186/s40364-023-00469-6
[25] Rangel-Pozzo A, Yu PLI, LaL S, et al. Telomere architecture correlates with aggressiveness in multiple myeloma. Cancers (Basel). 2021;13(8):1969. doi:10.3390/cancers13081969
[26] Yu PLI, Wang Y, Tammur P, et al. Distinct nuclear Organization of Telomeres and Centromeres in monoclonal Gammopathy of undetermined significance and multiple myeloma. Cells. 2019;8(7):723. doi:10.3390/cells8070723***This article demonstrates that telomere profiles can be a biomarker in Multiple Myeloma.*
[27] Klewes L, Vallente R, Dupas E, et al. Three-dimensional nuclear telomere organization in multiple myeloma. Transl Oncol. 2013;6(6):749–756. IN36. doi:10.1593/tlo.13613
[28] Knecht H, Johnson N, Bienz MN, et al. Analysis by TeloView® Technology Predicts the Response of Hodgkin's Lymphoma to First-Line ABVD Therapy. Cancers (Basel). 2024;16(16):2816. doi:10.3390/cancers16162816**This article reports the first use of TeloView analysis for analyzing Multiple Myeloma cancer cells.*
[29] Knecht H, Kongruttanachok N, Sawan B, et al. Three-dimensional telomere signatures of Hodgkin-and Reed-Sternberg cells at diagnosis identify patients with poor response to conventional chemotherapy. Transl Oncol. 2012;5(4):269–277. doi:10.1593/tlo.12142**This article demonstrated a clinical value of TeloView analysis and 3D telomere profiling as a prognostic marker in Hodgkin Lymphoma*
[30] Samassekou O, Hébert J, Mai S, et al. Nuclear remodeling of telomeres in chronic myeloid leukemia. Genes Chromosomes Cancer. 2013;52(5):495–502. doi:10.1002/gcc.22046
[31] Kumar S, Rajkumar SV, Jevremovic D, et al. Three-dimensional telomere profiling predicts risk of progression in smoldering multiple myeloma. Am J Hematol. 2024;99(8):1532–1539. doi:10.1002/ajh.27364
[32] Desitter I, Guerrouahen BS, Benali-Furet N, et al. A new device for rapid isolation by size and characterization of rare circulating tumor cells. Anticancer Res. 2011;31(2):427–441.***This article reports the development of a scoring model for Smoldering Multiple Myeloma, based on 3D telomere profiling*

[33] Vermolen B, Garini Y, Mai S, et al. Characterizing the three-dimensional organization of telomeres. Cytometry A. 2005;67(2):144–150. doi:10.1002/cyto.a.20159
[34] Hendricks A, Brandt B, Geisen R, et al. Isolation and enumeration of CTC in colorectal cancer patients: Introduction of a novel cell imaging approach and comparison to cellular and molecular detection techniques. Cancers (Basel). 2020;12(9):2643. doi:10.3390/cancers12092643**A pioneering study describing quantitative analysis of key telomere parameters*
[35] Theil G, Bialek J, Weiß C, et al. Strategies for isolating and propagating circulating tumor cells in men with metastatic prostate cancer. Diagnostics. 2022;12(2):497. doi:10.3390/diagnostics12020497
[36] Mehtar A, Wechsler J, Desterke C, et al. Optimizing Detection of Circulating Tumor Cells in Breast Cancer: Unveiling New Markers for Clinical Applications. Int J Mol Sci. 2025;26(10):4714. doi:10.3390/ijms26104714
[37] Chudasama D, Barr J, Beeson J, et al. Detection of circulating tumour cells and survival of patients with non-small cell lung cancer. Anticancer Res. 2017;37(1):169–173. doi:10.21873/anticanres.11302
[38] Rawal S, Ao Z, Agarwal A. מדה ומ אמייק רוזחמב לודיג יאתב רורחש תדיבל. Journal of Visualized Experiments. (JoVE). 2016(116):e54435.
[39] Yu J, Caragine T, Chen S, et al. Protection of human breast cancer cells from complement-mediated lysis by expression of heterologous CD59. Clin Exp Immunol. 1999;115(1):13–18. doi:10.1046/j.1365-2249.1999.00751.x
[40] Ganesan S, Palani HK, Balasundaram N, et al. Combination lenalidomide/bortezomib treatment synergistically induces calpain-dependent ikaros cleavage and apoptosis in myeloma cells. Mol Cancer Res. 2020;18(4):529–536. doi:10.1158/1541-7786.MCR-19-0431
[41] Kumar S, Paiva B, Anderson KC, et al. International Myeloma Working Group consensus criteria for response and minimal residual disease assessment in multiple myeloma. Lancet Oncol. 2016;17(8):e328–e346. doi:10.1016/S1470-2045(16)30206-6
[42] Chuang TCY, Moshir S, Garini Y, et al. The three-dimensional organization of telomeres in the nucleus of mammalian cells. BMC Biol. 2004;2(1):12. doi:10.1186/1741-7007-2-12**Currently accepted IMWG guidelines for Minimal residual disease assessment*
[43] Maciejowski J, de Lange T. Telomeres in cancer: tumour suppression and genome instability. Nat Rev Mol Cell Biol. 2017;18(3):175–186. doi:10.1038/nrm.2016.171
[44] De Lange T. editor Telomere-related genome instability in cancer. Cold Spring Harbor Symp Quant Biol. 2005;70:197–204. Cold Spring Harbor Laboratory Press. doi:10.1101/sqb.2005.70.032
[45] Mai S. editor 3D nuclear organization and genomic instability in cancer. BMC Proc. 2013;7 Suppl 2(Suppl 2):K17. Springer. doi:10.1186/1753-6561-7-S2-K17
[46] Gadji M, Mathur S, Bélanger B, et al. Three-dimensional nuclear telomere profiling as a biomarker for recurrence in oligodendrogliomas: a pilot study. Int J Mol Sci. 2020;21(22):8539. doi:10.3390/ijms21228539***A crucial paper discussing the link between telomere profiles and genomic instability as a hallmark of cancer*
[47] Wark L, Klonisch T, Awe J, et al. Dynamics of three-dimensional telomere profiles of circulating tumor cells in patients with high-risk prostate cancer who are undergoing androgen deprivation and radiation therapies. Urol Oncol. 2017;35(3):112.e1–112.e11. editors Elsevier. doi:10.1016/j.urolonc.2016.10.018
[48] Wark L, Danescu A, Natarajan S, et al. Three-dimensional telomere dynamics in follicular thyroid cancer. Thyroid. 2014;24(2):296–304. doi:10.1089/thy.2013.0118
[49] Kumar S, Rajkumar V, Jevremovic D, et al. P975: Three-dimensional telomere profiling predicts risk of relapse in newly diagnosed multiple myeloma patients. Hemasphere. 2023;7(S3):e07945f9. doi:10.1097/01.HS9.0000970804.07945.f9
[50] Zhang L, Beasley S, Prigozhina NL, et al. Detection and Characterization of Circulating Tumour Cells in Multiple Myeloma. J Circ Biomark. 2016;5:10. doi:10.5772/64124
[51] Andree KC, van Dalum G, Terstappen LW. Challenges in circulating tumor cell detection by the CellSearch system. Mol Oncol. 2016;10(3):395–407. doi:10.1016/j.molonc.2015.12.002
[52] Werner SL, Graf RP, Landers M, et al. Analytical Validation and Capabilities of the Epic CTC Platform: Enrichment-Free Circulating Tumour Cell Detection and Characterization. J Circ Biomark. 2015;4:3. doi:10.5772/60725
[53] Szalat RE, Anderson KC, Munshi NC. Role of minimal residual disease assessment in multiple myeloma. Haematologica. 2024;109(7):2049–2059. doi:10.3324/haematol.2023.284662
[54] Ding H, Xu J, Lin Z, et al. Minimal residual disease in multiple myeloma: current status. Biomark Res. 2021;9(1):75. doi:10.1186/s40364-021-00328-2
[55] Zamagni E, Tacchetti P, Barbato S, et al. Role of imaging in the evaluation of minimal residual disease in multiple myeloma patients. J Clin Med. 2020;9(11):3519. doi:10.3390/jcm9113519
[56] Messiou C, Porta N, Koh D-M, et al. Whole body MRI by MY-RADS for imaging response assessment in multiple myeloma. Blood Cancer J. 2025;15(1):122. doi:10.1038/s41408-025-01327-4
[57] Yanamandra U, Kumar SK. Minimal residual disease analysis in myeloma–when, why and where. Leuk Lymphoma. 2018;59(8):1772–1784. doi:10.1080/10428194.2017.1386304
[58] Kaedbey R, Knecht H, Anderson KC, et al. Preliminary results of 3D telomeres profiling for myeloma MRD and evaluation of concordance between blood and marrow. J Clin Oncol. 2025;43:e19560. doi:10.1200/JCO.2025.43.16_suppl.e19560

[59] Thiago LS, Perez-Andres M, Balanzategui A, et al. Circulating clonotypic B cells in multiple myeloma and monoclonal gammopathy of undetermined significance. Haematologica. 2014;99(1):155–162. doi:10.3324/haematol.2013.092817
[60] Paiva B, Vídriales MB, Rosiñol L, et al. A multiparameter flow cytometry immunophenotypic algorithm for the identification of newly diagnosed symptomatic myeloma with an MGUS-like signature and long-term disease control. Leukemia. 2013;27(10):2056–2061. doi:10.1038/leu.2013.166
[61] Muz B, de la Puente P, Azab F, et al. A CD138-independent strategy to detect minimal residual disease and circulating tumour cells in multiple myeloma. Br J Haematol. 2016;173(1):70–81. doi:10.1111/bjh.13927
[62] Rashid A, Wesson W, Abdallah AO, et al. BCMA-Directed MRD Detection as a Predictor of Relapse after BCMA CAR T in Multiple Myeloma. Clin Lymphoma Myeloma Leuk. 2025;25(1):52–57. doi:10.1016/j.clml.2024.10.003
[63] Morandi F, Horenstein AL, Costa F, et al. CD38: A Target for Immunotherapeutic Approaches in Multiple Myeloma. Front Immunol. 2018;9:2722. doi:10.3389/fimmu.2018.02722